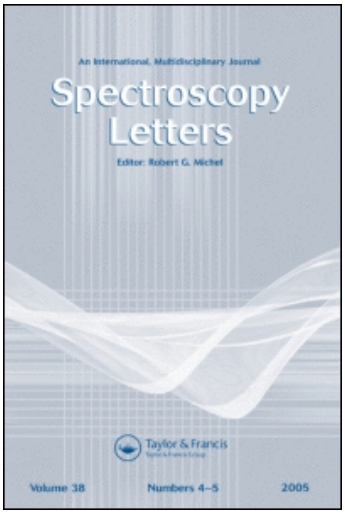

Spectroscopy Letters
Publication details, including instructions for authors and subscription information:
http://www.informaworld.com/smpp/title~content=t713597299

Characterization of Mango Juice by High-Resolution NMR, Hyphenated NMR, and Diffusion-Ordered Spectroscopy

Iola F. Duarte[a]; Brian J. Goodfellow[a]; Ana M. Gil[a]; Ivonne Delgadillo[b]
[a] CICECO, Department of Chemistry, University of Aveiro, Aveiro, Portugal [b] QOPNAA, Department of Chemistry, University of Aveiro, Aveiro, Portugal

To cite this Article Duarte, Iola F. , Goodfellow, Brian J. , Gil, Ana M. and Delgadillo, Ivonne(2005) 'Characterization of Mango Juice by High-Resolution NMR, Hyphenated NMR, and Diffusion-Ordered Spectroscopy', Spectroscopy Letters, 38: 3, 319 — 342
To link to this Article: DOI: 10.1081/SL-200058713
URL: http://dx.doi.org/10.1081/SL-200058713

Spectroscopy Letters, 38: 319–342, 2005

ISSN 0038-7010 print/1532-2289 online
DOI: 10.1081/SL-200058713

Characterization of Mango Juice by High-Resolution NMR, Hyphenated NMR, and Diffusion-Ordered Spectroscopy

Iola F. Duarte, Brian J. Goodfellow, and Ana M. Gil
CICECO, Department of Chemistry, University of Aveiro, Aveiro, Portugal

Ivonne Delgadillo
QOPNAA, Department of Chemistry, University of Aveiro, Aveiro, Portugal

Abstract: The application of nuclear magnetic resonance (NMR) spectroscopy, hyphenated NMR, and diffusion-ordered spectroscopy (DOSY) to the characterization of mango juice, as an example of a complex food mixture, is described. The compositional changes taking place as a function of ripening were followed, and selected metabolites were quantified by integration of the corresponding NMR peaks. In this way, an overall view of the metabolite changes is obtained, enabling the study of the biochemical mechanisms involved in the ripening process. More than 50 compounds were identified by 1D- and 2D-NMR, but many ambiguous assignments remain due to spectral overlap or insufficient coupling information. The use of Liquid Chromatography (LC-NMR) and LC-NMR/Mass Spectrometry (MS) enables a fuller characterization of the soluble pectin fraction to be made; its dependence on ripening stage is discussed. Finally, DOSY adds information on the M_r of many metabolites, including the pectin fractions of ripe and unripe mango juices, and enables further peak assignments to be made.

Keywords: DOSY, juice, LC-NMR, NMR, ripening

Received 8 May 2004, Accepted 21 October 2004

This paper was by special invitation as a contribution to a special issue of the journal entitled "Application of Spectroscopic Methods to Environmental Problems." The special issue was organized by Professor Peter A. Tanner, Professor in the Department of Biology and Chemistry at City University of Hong Kong.

Address correspondence to Ana M. Gil, CICECO, Department of Chemistry, University of Aveiro, 3810-193 Aveiro, Portugal. E-mail: agil@dq.ua.pt

INTRODUCTION

The current paper presents an overview of some of the ways in which nuclear magnetic resonance (NMR) spectroscopy may aid the assignment of compounds in complex mixtures (e.g., liquid foods such as fruit juices and other beverages, wine, and beer). The application of NMR to complex mixture analysis has been described at length for biofluids in the context of the early diagnosis of different diseases.[1–3] In complex food mixtures, high-resolution NMR has been increasingly applied, as shown by several recent references in the area.[4–9] In general, NMR of complex mixtures allows the detection of many different compounds through the analysis of only one sample requiring little or no preparation and, therefore, avoiding procedures that may interfere and change the original nature of the sample. NMR may also offer analytical rapidity, as a 1D spectrum may be recorded in a few minutes and automation may be implemented when analyzing high numbers of samples. However, NMR is an inherently insensitive technique and, in addition, ^{1}H-NMR spectra of complex mixtures are typically characterized by extensive signal overlap, even in 2D-NMR. This calls, in many cases, for more sophisticated techniques such as hyphenated NMR (LC-NMR or LC-NMR/MS) or diffusion-ordered spectroscopy (DOSY), the latter being based on the measurement of compound diffusivities. Recent applications of these techniques to several liquid foods may be found in Refs. 10 to 13.

This paper describes the use of high-resolution NMR, hyphenated NMR, and DOSY for the characterization of a fruit juice and the changes occurring upon fruit ripening. Mango juice is chosen as an example because, as a tropical food often imported, the detailed knowledge of its biochemistry (e.g., ripening, spoilage, contamination effects) is of importance in order to achieve adequate quality control. Some work has already been reported on the NMR of mango and its potential to characterize qualitative compositional changes associated with ripening and spoilage.[6,7] This paper addresses the effects of ripening alone and presents a more complete qualitative account of compounds detected, as well as quantification of some of those compounds. The complementarities of NMR, hyphenated NMR, and DOSY in aiding spectral assignment are discussed.

MATERIALS AND METHODS

Mangoes of the Tommy Atkins cultivar grown in Brazil were used. Fruits were directly air-freighted to Portugal and obtained from a commercial source, 3–4 days after harvest. The fruits were ripened at $22 \pm 1^{\circ}$C in natural light for 23 days, and 3 fruits were randomly selected every 2 days for firmness measurements and NMR analysis. The fruits showed signs of gradual ripening until day 19, after which over-ripening began. Juices were

prepared as follows: maceration of pulps in a domestic juice extractor, mixing of the 3 pulps, centrifugation (15 min, 15,000 rpm) and filtration through a glass microfiber filter under vacuum. Sodium azide (0.05%) was added before freezing the samples in N_2(l) and storing at -20°C until NMR analysis. After thawing, sample pH was adjusted to 6.0 with a sodium phosphate buffer, and D_2O and sodium 3-(trimethylsilyl)propionate (TSP) were added to obtain 8% D_2O and 0.02% TSP in the final sample.

The NMR spectra of juices were recorded at 27°C on a Bruker Avance DRX-600 spectrometer, operating at 599.87 MHz for proton and 150.85 MHz for carbon. ^{1}H 1D spectra were acquired with 64 scans, 65,535 data points, 12,019.23 Hz spectral width, 2.73 s acquisition time, and 7 s relaxation delay (based on ^{1}H T_1 measurements to ensure quantitative peak areas). Water presaturation was carried out by low-power selective irradiation at the water frequency during 3 s of the relaxation delay.[14] Metabolite concentrations were quantified by integration of selected peak(s) relatively to the TSP signal (0.0 ppm). Calculations made use of the simple relationship $C_Y = F\ (A_Y \cdot M_Y/n_Y)\ (C_{TSP} \cdot n_{TSP}/M_{TSP})$, where C is concentration, F is dilution factor, A is area of the integrated signal, M is molecular mass, and n is number of protons contributing to the integrated signal.

The Total Correlation Spectroscopy (TOCSY) spectra were acquired in the phase-sensitive mode using time-proportional phase incrementation (TPPI) and the MLEV17 pulse sequence.[15] A total of 200 increments with 16 transients and 2048 data points were acquired with a spectral width of 6613.76 Hz in both dimensions. ^{1}H–^{13}C phase sensitive (echo/antiecho) heteronuclear single quantum correlation (HSQC) spectra were recorded with inverse detection and ^{13}C decoupling during acquisition.[16,17] Data points (2048) with 64 scans per increment and 300 increments were acquired with spectral widths of 7507.51 and 25,000.00 Hz in the ^{1}H and ^{13}C dimensions, respectively. 2D *J*-resolved spectra were measured with water presaturation,[18] using a spectral width of 10,000 Hz in the proton dimension and 39 Hz in the J dimension. For each of 128 transients, 8192 data points were acquired with 16 scans. For DOSY experiments, the juice samples were prepared to give 10% D_2O and 0.02% TSP-d_4. The 2D ^{1}H-DOSY spectrum was recorded on a Bruker Avance DRX-500 spectrometer operating at 500.13 MHz for proton and equipped with a pulse gradient unit capable of producing magnetic field pulse gradients of 53.5 G cm^{-1} in the z-direction. The experiment was performed using a bipolar pulse longitudinal eddy current delay pulse sequence (ledbpgs2spr, Bruker library); a series of 32 spectra of 8016 data points and 256 scans were collected. The pulse gradients were incremented from 2% to 95% of the maximum gradient strength in a linear ramp. The diffusion delay (Δ) was 200 ms, and the length of the square diffusion encoding gradient pulses (δ) was 3.0 ms; the gradient stabilization time was 2 ms and relaxation delay 2 s. The temperature was set and controlled to 303 K with an air flow of 535 L h^{-1}, in order to avoid any convection gradients due to sample heating during the experiments.

The high-performance liquid chromatography (HPLC) system consisted of a HP 1100 solvent delivery pump with vacuum degasser (Agilent, Waldbronn, Germany), a manual injector from Rheodyne, model 7725i (Cotati, CA, USA), equipped with a 1-mL sample loop, and a diode array detector from Bruker (Rheinstetten, Germany). HPLC-NMR measurements were carried out using a BPSU-35 interface coupled to a DRX 500 NMR spectrometer equipped with a $^{1}H/^{13}C$ 4-mm inverse Liquid Chromatography (LC) probe head (120 μL) from Bruker. The temporary sample storage unit (BPSU-35) was used for automated multiple NMR experiments overnight. For online Mass Spectrometry (MS) detection, an ESQUIRE-3000 ion trap mass spectrometer, equipped with an electrospray ion source, from Bruker Daltonics (Bremen, Germany) was used. Five percent of the eluent was split into the MS using a splitter from LC Packings (San Francisco, CA, USA). Both UV as well as MS were used to trigger the transfer of the HPLC fractions to the BPSU (for temporary storage) or directly to the NMR. For the study of mango juice carbohydrates, chromatographic separation was carried out at 35°C, using a 300 × 7.8 mm ION-300 column, containing a cation exchange polymer in the hydrogen ionic form, with a particle size of 5.0 μm. The mobile phase consisted of 0.0085N H_2SO_4 in D_2O. Injection volumes of 50–100 μL of juice and flow rates of 0.15–0.30 mL/min were used. The diode array detector was operated at 200 and 220 nm, for detection of sugars and organic acids, respectively. ^{1}H-NMR spectra were obtained at 500 MHz using the continuous-flow and the loop-sampling methods. Electrospray ionization (ESI) was carried out in positive mode, and mass spectra were acquired up to m/z 1500 after adding 50 μL/min of 20 mM aqueous sodium acetate solution to the splitted ratio of the eluent via a T-piece with a syringe pump.

RESULTS AND DISCUSSION

1D- and 2D-NMR Spectroscopy of Mango Juice: Qualitative and Quantitative Analysis

Figure 1 shows a 1D ^{1}H-NMR spectrum of a sample of mango juice recorded at high field (600 MHz). The predominance of glucose, sucrose, and fructose is expressed by the high-intensity peaks visible in the central region of the spectrum (3–5.5 ppm), but much detail is also observed in the aliphatic (0–3 ppm) and aromatic (6–10 ppm) regions. The strong signal overlap makes the use of 2D-NMR (e.g.,TOCSY, $^{1}H/^{13}C$ correlation, *J*-resolved) necessary, and Fig. 2 shows expansions of the TOCSY spectrum of the same sample. A complete list of identified compounds is shown in Table 1.

The high-field region (0–3.0 ppm) shows signals from organic acids and amino acids (Fig. 2a). The acids generally referred to as predominant in mango,[20] citric, malic, and succinic acids, are clearly observed but,

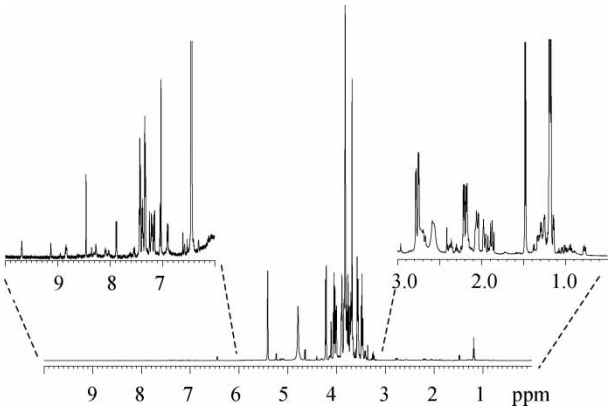

Figure 1. 600 MHz ^{1}H-NMR spectrum of ripe mango juice; 64 transients.

interestingly, shikimic and quinic acids also appear in relatively high amounts. Lesser amounts of lactic, propionic, and 3-hydroxybutyric acids are also identified. Alanine is the major aliphatic amino acid, as previously reported for different mango cultivars[21] and valine, leucine, isoleucine, threonine, glutamine, glutamic acid, and GABA are also detected. Arginine, aspartic acid, and asparagine may also be found in significant levels, depending on the origin of the mangoes, as shown by a comparative study (not shown) of fruits of the Haden variety from Venezuela and from Brazil. The presence of lipids is detected by the spin system at 0.89, 1.29, 1.55, and 2.21 ppm, which may arise from one or more saturated fatty acids (e.g. palmitic acid.[21]) Several overlapped signals in the 1.20–1.32 ppm region, correlated to resonances at 3.4–5.2 ppm, may be tentatively assigned to fucose and rhamnose H6 protons. It is known that α-rhamnose may be found in the free form or interspersed with galacturonic acid residues in pectic chains;[22] however, the high degree of spectral overlap in the midfield region hinders any objective interpretation. Other compounds detected in the high-field region are acetoin, isopropanol/2,3-butanediol, and ethanol; these are typical fermentation products that may reflect some ongoing microbial activity. This has been observed in a range of samples, although ethanol often gives much weaker signals, and acetoin and isopropanol/2,3-butanediol are not usually detected.

The midfield region (3.0–5.5 ppm) is dominated by intense and overlapped signals of the major sugars easily recognizable in the anomeric region (Fig. 1) at 4.11, 4.64, 5.23, 5.41 ppm, respectively, for fructose (H3 and H4 of β-fructofuranose), β-glucose (H1), α-glucose (H1), and sucrose (H1 of the glucose ring). Several weak signals are also visible at 4.5–5.5 ppm (Fig. 2b), indicating the presence of xylose and of arabinose and/or galactose. The broad signals at 5.05–5.20 ppm may arise from

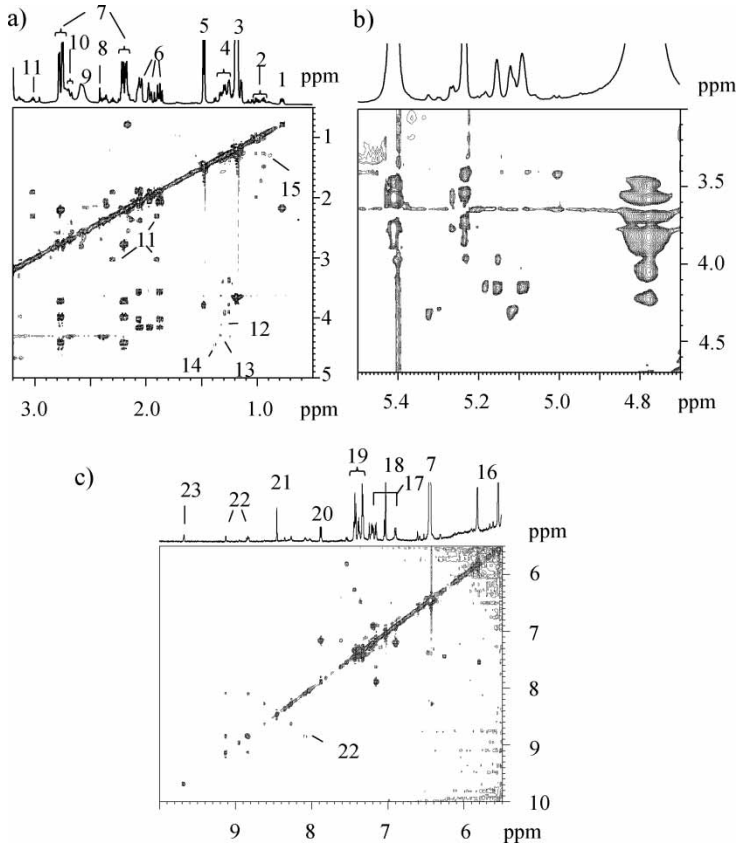

Figure 2. TOCSY spectrum of ripe mango juice: (a) high-field region: 1, TSP; 2, val,leu.ile; 3, ethanol; 4, rha/fuc; 5, ala; 6, quinic; 7, shikimic acid; 8, succinic acid; 9, citric acid; 10, malic acid; 11, GABA; 12, lactic acid; 13, thr; 14, acetoin. (b) Mid-field region and (c) low-field region: 16, uracyl; 17, tyr; 18, gallic acid; 19, phe; 20, unknown; 21, formic acid; 22, niacin; 23, acetaldehyde.

pectic nonreducing galacturonic acid (GalA) residues, namely H1 protons of nonesterified GalA and H5 protons of esterified (methylated) GalA.[23,24] However, with the exception of a spin system seen for a broad weak peak at 5.32 ppm, indicative of reducing α-GalA, no other GalA spin systems could be identified.

In the low-field region (5.5–10 ppm), the most prominent signal belongs to shikimic acid (Fig. 2c). Other compounds readily identified are tyrosine, phenylalanine, acetaldehyde, and niacin. However, many signals remain unassigned objectively; for example, the singlets tentatively attributed to fumaric acid (6.52 or 6.61 ppm), gallic acid (7.03 or 7.04 ppm), adenine or adenosine (8.27 and 8.35 ppm), and formic acid (8.45 ppm). In addition, it has been seen

Table 1. NMR data based on 1D- and 2D-NMR of mango juice: ^{1}H and ^{13}C chemical shifts, ^{1}H multiplicity and J_{HH}

Compound	Assignment	δ ^{1}H (ppm)	Multiplicity	J (Hz)	δ ^{13}C (ppm)
Acetaldehyde	CH_3	2.24	d	3.0	
	CH	9.68			
Acetaldehyde hydrate	CH_3, hydrate	1.33			
	CH, hydrate	5.25			
Acetate	βCH_3	1.92	s		
Acetoin	CH_3	1.38	d	7.0	
	CH	4.43			
Adenine/adenosine[a]	C8H, ring	8.27	s		
	C2H, ring	8.35	s		
Alanine	βCH_3	1.48	d	7.2	17.00
	αCH	3.78			51.53
γ-Aminobutyric acid (GABA)	βCH_2	1.90			24.14
	αCH_2	2.30	t	7.4	34.52
	γCH_2	3.01	t	7.4	40.20
α-Arabinose/α-Galactose[a]	C2H	3.80			
	C3H	3.90			
	C1H	5.30	d	3.4	
β-Arabinose/β-Galactose/	C1H	3.46, 4.55			
β-Galacturonic acid/β-Fucose[a]	C2H	3.52, 3.70, 4.57			
	C3H	3.52, 4.51			
Arginine	γCH_2	1.69	m		
	βCH_2	1.91			
	δCH_2	3.25			

(*continued*)

Table 1. Continued

Compound	Assignment	δ ^{1}H (ppm)	Multiplicity	J (Hz)	δ ^{13}C (ppm)
Asparagine	βCH	2.85	dd	7.6; 16	35.51
	β'CH	2.95	dd	4.0; 16	
	αCH	4.01			
Aspartic acid	βCH	2.69	dd	7.6; 16	37.29
	β'CH	2.83	dd	3.6; 16	
	αCH	3.92			
2,3-Butanediol/Isopropanol	CH_3	1.14	d	6.0	
	CH	3.68			
Citric acid	α, γCH	2.56	d	1.52	45.22
	α', γ' CH	2.66	d	15.2	
Ethanol	CH_3	1.18	t	7.1	19.20
	CH_2	3.65			
Fatty acids (saturated)	ωCH_3	0.89	t	7.5	
	$\underline{CH_2}$-CH_3	1.29			
	$\underline{CH_2}$-CH_2-CH_3	1.55			
	$\underline{CH_2}$-COOH	2.21			
Formic acid[a]	$\underline{H}$COOH	8.45	s		
Fructose (β-furanose)	C6H	3.68			
	C5H	3.82			
	C3H, C4H	4.11			76.71

α-Fucose[a]	C6H	1.20			
	C3H/C4H	3.66			
	C2H	3.76			
	C5H	4.22			
	C1H	5.21			
β-Fucose[a]	C6H	1.29			
	C4H	3.59			
	C5H	3.77			
Fumaric acid[a]	CH	6.52 or 6.61	s		
α-Galacturonic acid (free/pectic, reducing end)[a]	C2H	3.88			
	C3H	4.00			
	C4H	4.31			
	C1H	5.32	Broad		99.30
α-Galacturonic acid (pectic, nonreducing)/α-Rhamnose[a]	un.	5.06 [3.98/4.09]			98.44
	un.	5.09 [4.03/4.15/4.23]			100.00/108.35
	un.	5.12 [4.09/4.30]			98.56
	un.	5.15 [3.75/3.97/4.15]			107.95
	un.	5.18 [4.00/4.12]			107.63
Gallic acid[a]	C2H, C6H	7.03 or 7.04	s		
α-Glucose	C4H	3.41			
	C2H	3.54			
	C3H	3.71			
	C5H, C6H	3.77–3.88			
	C1H	5.23	d	3.6	93.42

(*continued*)

Table 1. Continued

Compound	Assignment	δ ^{1}H (ppm)	Multiplicity	J (Hz)	δ ^{13}C (ppm)
β-Glucose	C2H	3.25			
	C4H	3.41			
	C5H	3.45			
	C3H	3.48			
	C6H	3.73, 3.90			
	C1H	4.65	d	8.0	97.52
Glutamic acid	β, β'CH	2.05			
	γCH_2	2.37			
	αCH	3.76			
Glutamine	βCH_2	2.13			
	γCH_2	2.35			
	αCH	3.76			
β-Hydroxybutyric acid	γCH_3	1.20			
	αCH	2.31			
	α'CH	2.41			
	βCH	4.13			
Isoleucine	δCH_3	0.94	t	7.3	
	$\gamma' CH_3$	1.01	d	7.0	15.40
	γCH	1.25			
	γ'CH	1.48			
	βCH	1.98			
Lactic acid	βCH_3	1.32	d	7.0	20.80
	αCH	4.10			69.00
Leucine	δ, $\delta' CH_3$	0.96			21.61, 22.89
	βCH_2, γCH	1.71			

Malic acid	βCH	2.38	dd	7; 16.5	42.07
	β′CH	2.68			
	αCH	4.30			70.31
Methanol	CH_3	3.35	s		49.75
Myo-inositol	C5H	3.28			
	C1H, C3H	3.53			
	C4H, C6H	3.63			
	C2H	4.06			
Niacin	C5H	8.08			
	C4H, C6H	8.84			
	C2H	9.12	s		
Phenylalanine	βCH	3.12			
	β′CH	3.28			
	αCH	3.97			
	C3H, C5H ring	7.33	m		129.93
	C4H	7.38	m		
	C2H, C6H ring	7.43	m		129.74
Polyphenols or Gultamine[c]	un.	6.9	Broad		
	un.	7.6	Broad		
Propionic acid	βCH_3	1.08	t	7.1	
	αCH_2	2.40			
Quinic acid	$\alpha CH_2/\varepsilon CH_2$	1.84–2.10			38.25
	βCH	3.55	dd		
	δCH	4.02	dd		
	γCH	4.14	dd		

(*continued*)

Table 1. Continued

Compound	Assignment	δ ^{1}H (ppm)	Multiplicity	J (Hz)	δ ^{13}C (ppm)
α-Rhamnose (free/pectic)[a,b]	un.	1.22, 3.42, 3.88			16.23
	un.	1.24, 3.48, 3.58			17.33
	un.	1.25, 3.35, 3.78, 3.86, 4.03			19.20
	un.	1.29, 3.48, 3.87			
β-Rhamnose[a]	C6H	1.31			17.45
	C5H	3.40			
Shikimic acid	C7H	2.19	dq		33.15
	C7H′	2.77	dd		
	C5H	3.70			
	C6H	3.98			
	C4H	4.40	t		72.10
	C3H	6.44			132.30
Succinic acid	α, βCH$_2$	2.41	s		32.24
Sucrose	G4H	3.47			
	G2H	3.57			
	G3H	3.78			
	G5H, G6H	3.84			
	G1H	5.41	d	3.6	93.00
	F6H	3.82			
	F5H	3.88			
	F4H	4.05			
	F3H	4.22	d	8.7	75.47

Threonine	γCH_3	1.32	d	5.2	20.80
	αCH	3.61			
	βCH	4.26			
Tyrosine	C3H, C5H ring	6.90	d	8.5	
	C2H, C6H ring	7.19	d	8.5	
Uracil	C5H	5.80	d		
	C6H	7.54	d		
Uridine	C4′H	4.11			
	C3′H	4.21			
	C2′H	4.38			
	C5H ring	5.88	d	8.2	105.00
	C1′H	5.89			90.51
	C6H ring	7.85	d	8.2	144.56
Valine	γCH_3	0.98	d	7.0	17.39
	$\gamma' CH_3$	1.04	d	7.0	18.70
	βCH	2.27			29.73
β-Xylose[a]	C2H	3.26			
	C3H	3.39			
	C4H	3.64			
	C1H	4.61			

s, singlet; d, doublet; t, triplet; q, quartet; dd, doublet of doublets; dq, doublet of quartets; m, multiplet; un, unassigned.

[a]Tentative identification.

[b]The ^{13}C signals indicated are coupled to the ^{1}H signals at 1.22–1.25 ppm and arise from C6H.

[c]See text for discussion. The nomenclature followed for amino acids is based on Reference.[19]

that juices from different batches often show two typical broad correlated resonances at 6.89 and 7.61 ppm (Fig. 3b). Two possible assignments have been suggested for these peaks: (1) polyphenolic species, based on studies of apple juice under varying conditions of air exposure and polyphenoloxidase activity[25] and (2) slowly exchanging glutamine NH protons, based on D_2O exchange studies.[9] It will be shown below that DOSY of mango juice gives results that support the latter assignment.

Figure 3 shows the aliphatic and aromatic regions of the spectra of mango juices collected from a second sample batch at days 1, 7, and 19 of ripening. The high-field region (Fig. 3a) shows clear variations in the organic acid and amino acid profile. In agreement with several reports,[20,26] citric acid is abundant in unripe juices (ap. 14 g/L) and rapidly declines during ripening to levels below 3 g/L (Fig. 4a), presumably due to its utilization as a respiratory substrate. This rapid citric acid loss accounts for most of the acidity decrease observed during ripening. Quinic, shikimic, malic, and succinic acids are present through all ripening stages and show smaller variations. Malic acid shows a small loss until day 13 (Fig. 4a) and then an increase until day 23 to concentrations close to 1.6 g/L, in agreement with previous HPLC measurements.[26] Shikimic acid decreases steadily from 1.9 g/L to 1.2 g/L (Fig. 4b), and succinic and quinic acids concentrations could not be determined due to signal overlap in most spectra. In terms of amino acid composition, the most drastic change is the decrease of arginine, in contrast with increases in valine, leucine, isoleucine, alanine, asparagine, glutamine, and γ-aminobutyric acid (GABA) (Fig. 4c). After arginine, alanine is the second most abundant

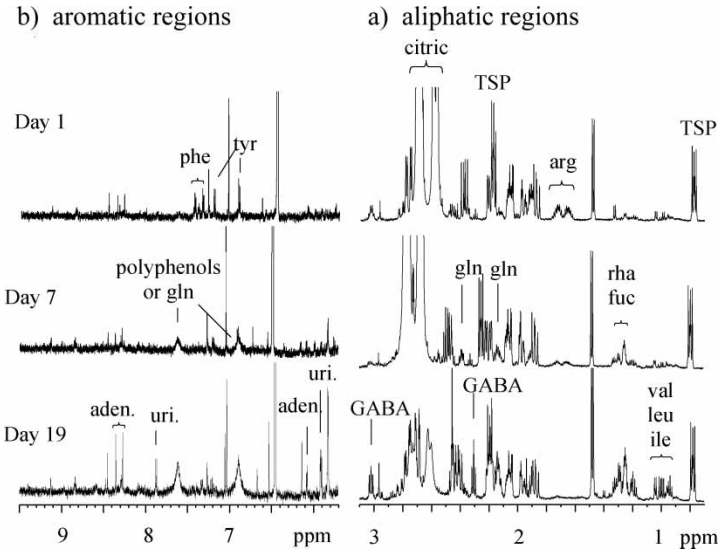

Figure 3. (a) Aliphatic and (b) aromatic regions of the ^{1}H-NMR spectra of mango juice for days 1, 7, and 19 of ripening; uri., uridine; aden., adenosine.

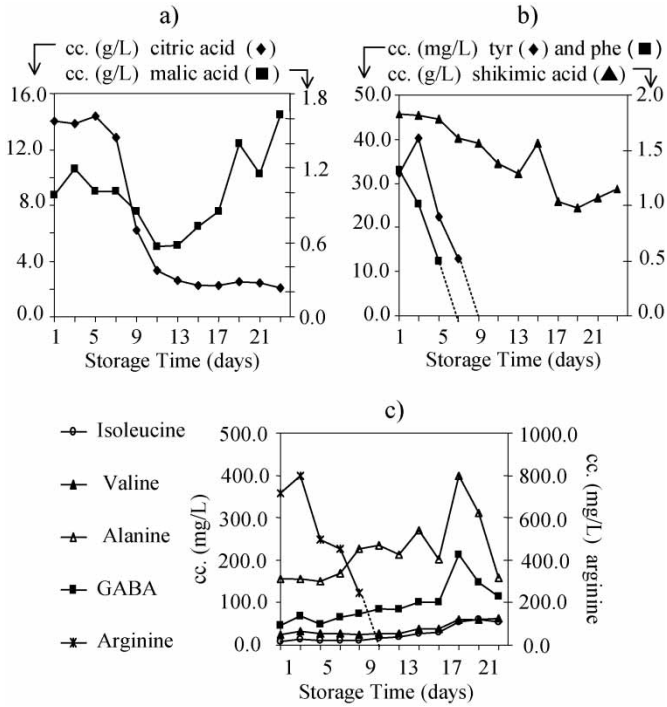

Figure 4. Variations in mango juice composition during ripening: (a) citric (2.58 ppm) and malic (2.40) ppm acids, (b) tyr (7.19 ppm), phe (7.30–7.45 ppm) and shikimic acid (6.45 ppm), (c) ile (1.01 ppm), val (1.04 ppm), ala (1.48 ppm), GABA (2.30 ppm), arg (1.60–1.78 ppm). Dashed lines indicate undetectable amounts.

amino acid at the beginning of ripening, showing a slight increase throughout, similarly to GABA. Isoleucine and valine increase 6-fold and 2.5-fold, respectively. Interestingly, phenylalanine and tyrosine are used up early in the ripening process. The possible involvement of these amino acids, and possibly of shikimic acid (Fig. 4b), as precursors for phenolic polymerization may be suggested. Unfortunately, if the broad signals at 6.89 and 7.61 (Fig. 3b) do not arise from polyaromatic species but rather from glutamine, no direct indicator of polyphenols is visible in the spectra.

The concentrations of the three main sugars vary significantly with ripening stage (Fig. 5). Sucrose, α-glucose, and β-glucose were quantified through the 5.41 (H1, glucose ring), 5.23 (H1), and 4.64 (H1) ppm peaks, respectively. For fructose, the 4.11 ppm peak (H3 and H4 of β-furanose form) was used and a proportion of 65% β-pyranose/25% β-furanose assumed for calculation of total fructose, based on sugar solution studies at 31°C.[27] On day 1, fructose predominates (Fig. 5a) but, after day 5, sucrose becomes the most abundant sugar, reaching a concentration almost 5-fold

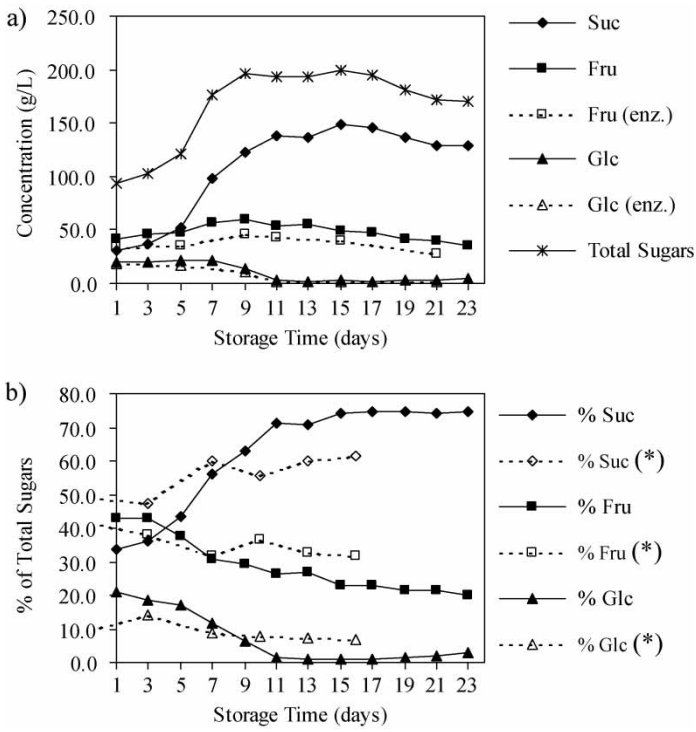

Figure 5. Sugar variations in mango juice during ripening: (a) concentrations (g/L) determined for sucrose (5.41 ppm), fructose (4.11 ppm), α-glcucose (5.23 ppm), and β-glcucose (4.64 ppm) by NMR and by enzymatic methods for glucose and fructose; (b) relative contribution of each sugar to total sugar content. (*) Results reported in Ref.[26].

higher than in day 1. Glucose shows a 7.5-fold decrease after day 7, and fructose does not vary much throughout the ripening process. Fructose amounts calculated by NMR are slightly overestimated compared to the reference enzymatic values (Fig. 5a), possibly due to signal overlap and/or temperature-induced changes in the pyranose/furanose ratio. The contributions of each sugar to the total sugar content are shown in Fig. 5b. In unripe juice, sucrose, fructose, and glucose account for approximately 34%, 43%, and 21% of total sugars, respectively, whereas in ripe juice, sucrose reaches 75%, fructose 20–23%, and glucose less than 2–3%. These results are in agreement with those obtained by HPLC for juices of the same mango cultivar, shown in Fig. 5b.[26]

Additional considerations include an apparent increase of nonreducing GalA (5.05–5.20 ppm) during ripening, which, along with an intensity increase for rhamnose/fucose signals at 1.20–1.30 ppm, indicates an increase in pectic oligosaccharides detected in the juice, as a result of pectin

hydrolysis. In the low-field region, uridine and adenosine are seen to increase in the latter stages of ripening and other spectral changes regard unassigned signals (e.g., increases at 5.82, 6.13, and 7.05 ppm and decrease at 7.26 ppm).

Hyphenated NMR Spectroscopy of Mango Juice

In the current section, a more complete characterization of the less abundant carbohydrates observed as low intensity peaks at 5.2–5.4 ppm (Fig. 2b) is attempted by hyphenated NMR. Figure 6 shows the continuous-flow NMR chromatogram obtained by the elution of ripe mango juice in an ION-300 column. The vertical lines at a 4.7 and 2.0 ppm arise, respectively, from water and residual acetonitrile. Between retention times (RT) of 15 and 30 min, the elution of the major sugars and organic acids occurs. Sucrose starts eluting at about 15.0 min and is followed by glucose (line 2 shows co-elution of both sugars). Glucose co-elutes with fructose and citric acid in line 3; fructose and malic acid elute together at 24.0 min in line 4, followed by shikimic acid in line 5. This is confirmed by the corresponding MS spectra (not shown). The pectic fraction elutes at earlier RTs (line 1), potentially enabling a more detailed characterization of these carbohydrates. Unfortunately, no MS data is available, because this fraction showed no ionization under the conditions used. In order to improve the S/N of the 1D spectrum of line 1, a second chromatographic was run, during which the pectic fraction was collected into a capillary loop, for subsequent 1D- and 2D-NMR characterization. Figure 7 shows the spectra of the pectic fractions thus obtained for unripe and ripe mango juices and for which 2D-NMR experiments were

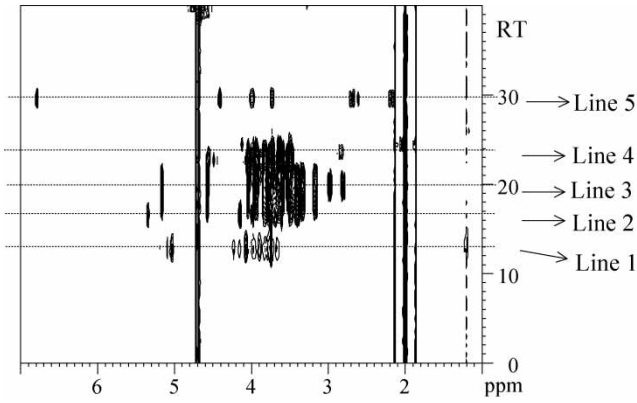

Figure 6. Continuous-flow NMR chromatogram resulting from the elution of mango juice on a ION-300 column (flow rate 0.3 mL/min). Compounds identified in lines 1 to 5:1, pectic fraction (no MS ionisation); 2, sucrose + glucose; 3, glucose + fructose + citric acid; 4, fructose + malic acid; and 5, shikimic acid.

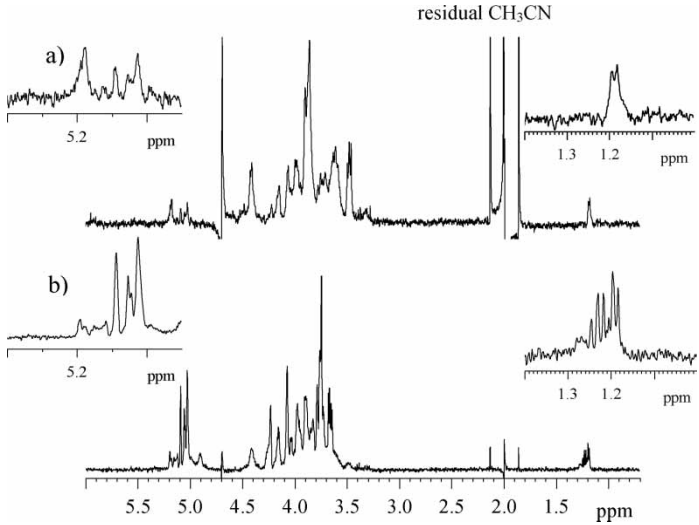

Figure 7. ^{1}H-NMR spectra obtained for the pectic fractions of (a) unripe and (b) ripe mango juices eluted on a ION-300 column (injection volume 50 μL); 128 transients.

performed (not shown). The profile of the bottom spectrum (ripe juice) shows two doublets at 1.19 and 1.22 ppm, readily assignable to methyl protons (H-6) of rhamnose units. A third overlapped signal at 1.23 ppm is identified as part of a second spin system also characteristic of rhamnose. Based on the ^{1}H chemical shifts reported for sugars[28] and for rhamnogalacturonan oligosaccharides,[29,30] these signals were assigned to α- and β-rhamnose in reducing chain ends and to nonreducing rhamnose (Table 2). The

Table 2. ^{1}H-NMR chemical shifts (ppm) obtained for the pectic fraction of ripe mango juice obtained by LC-NMR

	H-1	H-2	H-3	H-4	H-5	H-6
Rha (r.e.)						
α	5.12	4.06	3.80	3.41	3.83	1.22
β	4.88	n.i.	3.62	3.85	3.37	1.23
Rha (n.r.)	5.19	4.23	3.76	3.32	3.56	1.19
GalA possibly esterified	n.i.	n.i.	3.61	4.41	5.01	
	n.i.	n.i.	3.78	4.34	5.13	
	4.99	4.05	n.i.	n.i.	n.i.	
	5.02	4.05	n.i.	n.i.	n.i.	
	5.04	4.22	n.i.	n.i.	n.i.	
GalA nonesterified	5.09	4.06	3.87	n.i.	n.i.	
	5.15	4.09	3.88	n.i.	n.i.	

r.e., reducing end; n.r., nonreducing; n.i., not identified.

4.9–5.4 ppm region (Fig. 7) shows signals of at least five different GalA environments (Table 2). Of these, at least two are nonesterified (H-1 chemical shifts fall in the 5.1–5.2 ppm range), and the remaining are possibly esterified, based on correlations between 5.0–5.1 and 4.3–4.4 ppm assigned to H5 and H4, respectively. It also becomes apparent that reducing GalA is not present, as the H1 signals expected at 5.3 and 4.6 ppm for α- and β-GalA, respectively, are absent. Also, there is no clear evidence of the presence of neutral sugars other than rhamnose. The effect of ripening can be clearly seen in the spectral profiles of the two pectic fractions (Fig. 7). For unripe juice, lower S/N ratio and poorer resolution are observed, indicative of less pectic material and of larger molecules, respectively. Furthermore, the spectrum of unripe juice reveals the following: (1) only nonreducing rhamnose is present (1.19 ppm doublet), (2) the main signals at 3.0–4.5 ppm arise from β-galactose and/or β-arabinose, and (3) the GalA signals at 4.9–5.4 ppm are much weaker. Therefore, the less abundant pectic fraction of unripe juice contains larger molecules with nonreducing rhamnose units and higher contents of neutral sugars (galactose/arabinose), as expected based on the literature.[31] The above results show that pectin analysis may be achieved to some extent by hyphenated NMR, thus allowing the noninvasive characterization of the pectic fraction of fruits.

Diffusion-Ordered Spectroscopy of Mango Juice

The principle of DOSY is to separate NMR signals with basis on the diffusion coefficients of the corresponding compounds.[32–34] The potential interest of applying DOSY to complex mixtures such as fruit juices is to add to the assignment carried out by 1D- and 2D-NMR, using information on compound diffusivities and hence molecular weights. Figure 8 shows the DOSY spectrum of ripe mango juice where some assignments are indicated. The diffusivities of most signals in the aliphatic and aromatic regions fall in the 1×10^{-10} to $15 \times 10^{-10}\,m^2s^{-1}$ range and are readily interpretable based on the known assignments. However, some new information may be obtained. First, some assignments could be clarified in the low-field region based on the diffusivities shown: (1) the singlets at 7.08 ppm and 8.45 ppm were identified as gallic acid and formic acid, respectively, (2) the weaker DOSY peaks at 7.39 and 8.64 ppm are consistent with assignment to histidine, (3) the DOSY peaks at 8.25, 8.30, and 8.64 ppm may arise in part from adenine/adenosine, and (4) the broad resonances at 6.89 and 7.61 ppm in the spectra of some juice batches (Fig. 3b) are assigned to glutamine, and not to polyphenols, due to their relatively high diffusivity ($6.8 \times 10^{-10}\,m^2s^{-1}$). The second advance provided by DOSY relates to the pectic fraction and to the peaks indicated in Fig. 8a as pectic moieties. The signals at 1.2–1.3 ppm correspond to rhamnose moieties and seem to align,

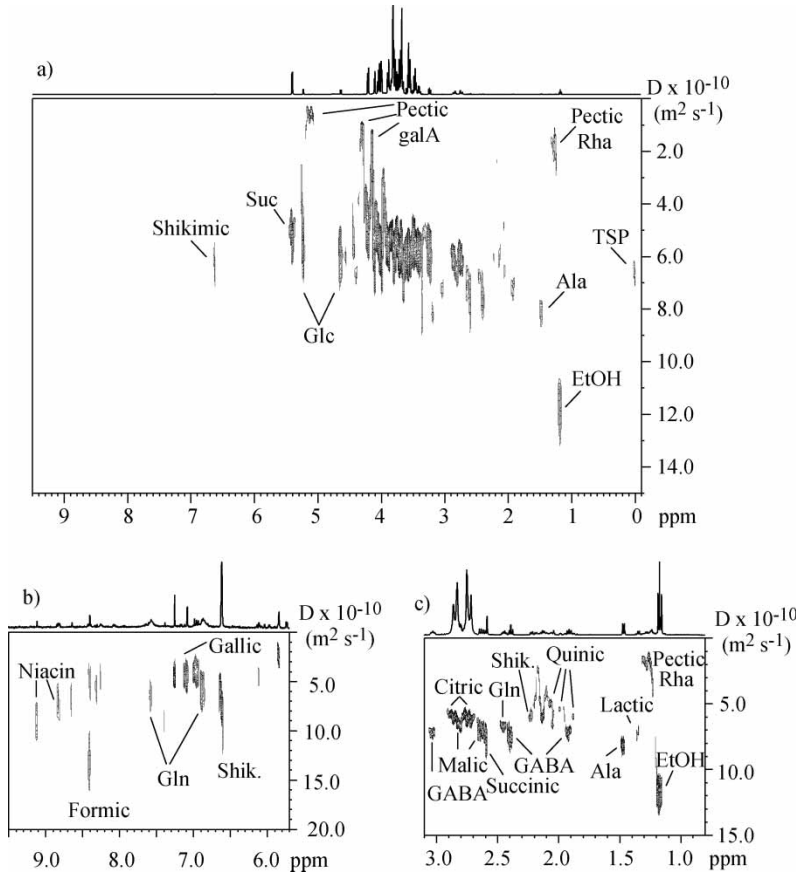

Figure 8. DOSY spectrum of ripe mango juice: (a) whole spectrum, (b) aromatic, and (c) aliphatic regions.

in part, with a weak signal at 5.19 ppm; based on Table 2, it may be seen that these signals correspond mainly to nonreducing rhamnose monomers. Because, for globular molecules of fixed density, the diffusion coefficient is inversely proportional to the cube root of relative molecular mass M_r, estimates of M_r were made using selected peaks as calibrants, for both ripe and unripe juices. The calibrants used were the DOSY peaks for TSP-d_4 (M_r 149, D $6.6 \times 10^{-10}\,m^2\,s^{-1}$), ethanol ($M_r$ 46, D $1.1 \times 10^{-9}\,m^2\,s^{-1}$), alanine ($M_r$ 89, D $8.2 \times 10^{-10}\,m^2\,s^{-1}$), citric acid ($M_r$ 192, D $6.0 \times 10^{-10}\,m^2\,s^{-1}$), glucose ($M_r$ 180, D $5.7 \times 10^{-10}\,m^2\,s^{-1}$), sucrose ($M_r$ 342, D $4.6 \times 10^{-10}\,m^2\,s^{-1}$), and shikimic acid ($M_r$ 174, D $6.6 \times 10^{-10}\,m^2\,s^{-1}$). With basis on this information, the average diffusivity of $1.7 \times 10^{-10}\,m^2\,s^{-1}$ observed for the rhamnose signals in ripe juice was found to indicate an average M_r of 1690. In addition, a clear signal is

observed at 5.10 ppm for GalA residues corresponding to slower diffusivity ($0.67 \times 10^{-10}\,m^2\,s^{-1}$) than that of the rhamnose signal. This reflects protons in different polymer molecules and, in fact, the estimated M_r for the GalA-rich polymers is 3976. Comparison of these results with those obtained for unripe juice (not shown) indicates slightly lower diffusivities, 1.5×10^{-10} and $0.52 \times 10^{-10}\,m^2\,s^{-1}$, for the equivalent rhamnose and GalA peaks, respectively. Because sample viscosity is comparable to that of ripe juice (TSP-d_4 diffusivity is 6.5×10^{-10} and $6.6 \times 10^{-10}\,m^2\,s^{-1}$ in unripe and in ripe juices, respectively), these values could be compared with those of ripe juice. The slightly slower diffusivities in the unripe stage correspond to estimated M_r of 1972 (rhamnose peak) and 4639 (GalA peak), suggesting the expected presence of larger segments, at an earlier stage of pectin hydrolysis. It should be noted, however, that these calculated M_r values carry a relatively high uncertainty (30–40%) and, thus, should be taken as simple estimates at this stage. Improved values of M_r may be obtained through the use of a calibration curve based on suitable pectin models with a range of molecular weights. These observations show that the DOSY technique can be used to follow the M_r evolution of pectic segments in solution as ripening proceeds.

CONCLUSIONS

The use of NMR spectroscopy for the qualitative and quantitative monitoring of the composition of mango juice during ripening has been described. The technique enables the identification of just over 50 compounds of varying natures and concentrations. As ripening proceeds, many compositional changes occur and, by signal integration, absolute concentrations were obtained for organic acids, amino acids, and sugars. In this way, the evolution of many different compounds throughout ripening may be characterized in a relatively rapid and simple manner, confirming the utility of NMR for the study of the specific biochemical mechanisms involved in ripening. The pectic fraction present in the juice is observable as broader signals in the aliphatic and sugar regions. Unambiguous characterization of these components by standard NMR is hindered by strong signal overlap; however, hyphenated NMR allows the separation and improved characterization of pectic fractions for both ripe and unripe juices. Finally, the diffusivity information provided by DOSY allowed some previous ambiguous assignments, such as some singlets in the aromatic region and the two broad signals in the same region, previously assigned to polyphenols and now attributed to glutamine, to be clarified. DOSY also proved to be of use in providing average M_r estimates for the pectic fraction of both unripe and ripe juices, reflecting the expected decrease in size as ripening and, hence, pectin hydrolysis, proceeds.

ACKNOWLEDGMENTS

The authors acknowledge Dr. Manfred Spraul, Dr. M. Godejohann, and Dr. U. Braunman, from Bruker Biospin GmbH, Germany, for support in the use of the hyphenated NMR equipment. I. Duarte acknowledges financial support provided by the Foundation for Science and Technology, Portugal, through the grant PRAXIS/BD/1566/98.

REFERENCES

1. Tate, A. R.; Foxall, P. J. D.; Holmes, E.; Moka, D.; Spraul, M.; Nicholson, J. K.; Lindon, J. C. Distinction between normal and renal cell carcinoma kidney cortical biopsy samples using pattern recognition of H-1 magic angle spinning (MAS) NMR spectra. *NMR in Biomedicine* **2000**, *13*, 64–71.
2. Bollard, M.; Holmes, E.; Lindon, J. C.; Nicholson, J. K. High-resolution H-1 and H-1-C-13 magic angle spinning NMR spectroscopy of rat liver. *Magn. Reson. Med.* **2000**, *44* (2), 201–207.
3. Lindon, J. C.; Nicholson, J. K.; Holmes, E.; Everett, J. R. Metabonomics: metabolic processes studied by NMR spectroscopy of biofluids. *Concepts Magn. Reson.* **2000**, *12* (5), 289–320.
4. Bosco, M.; Toffanin, R. D.; de Palo Zatti, L.; Segre, A. L. High-resolution H-1 NMR investigation of coffee. *J. Sci. Food Agric.* **1999**, *79*, 869–878.
5. Lakenbrink, C.; Engelhardt, U. H.; Wray, V. J. Identification of two novel proanthocyanidins in green tea. *J. Agric. Food Chem.* **1999**, *47*, 4621–4624.
6. Gil, A. M.; Duarte, I. F.; Delgadillo, I.; Colquhoun, I. J.; Casuscelli, F.; Humpfer, E.; Spraul, M. Study of the compositional changes of mango during ripening by nuclear magnetic resonance spectroscopy. *J. Agric. Food Chem.* **2000**, *48*, 1524–1536.
7. Duarte, I. F.; Delgadillo, I.; Gil, A. M. An NMR study of the biochemistry of mango: the effects of ripening, storage conditions and microbial growth. In *Magnetic Resonance in Food Science—A View to the Next Century*; Webb, G., Belton, P. S., Gil, A. M., Delgadillo, I., Eds.; Royal Society of Chemistry, London, 2001; pp. 259–266.
8. Duarte, I. F.; Barros, A.; Belton, P. S.; Righelato, R.; Spraul, M.; Humpfer, E.; Gil, A. M. High-resolution nuclear magnetic resonance spectroscopy and multivariate analysis for the characterization of beer. *J. Agric. Food Chem.* **2002**, *50*, 2475–2481.
9. Sobolev, A. P.; Segre, A.; Lamanna, R. Proton high-field NMR study of tomato juice. *Magn. Reson. Chem.* **2003**, *41* (4), 237–245.
10. Duarte, I. F.; Godejohann, M.; Braumann, U.; Spraul, M.; Gil, A. M. Application of NMR spectroscopy and LC-NMR/MS to the identification of carbohydrates in beer. *J. Agric. Food Chem.* **2003**, *51* (17), 4847–4852.
11. Gil, A. M.; Duarte, I. F.; Godejohann, M.; Braumann, U.; Spraul, M. Characterization of the aromatic composition of some liquid foods by nuclear magnetic resonance spectrometry and liquid chromatography with nuclear magnetic resonance and mass spectrometric detection. *Anal. Chim. Acta* **2003**, *488* (1), 35–51.

12. Gil, A. M.; Duarte, I. F.; Cabrita, E.; Goodfellow, B. J.; Spraul, M.; Kerssebaum, R. Exploratory applications of diffusion ordered spectroscopy (DOSY) to liquid foods: an aid towards spectral assignment. *Anal. Chim. Acta* **2004**, *506* (2), 215–223.
13. Nilsson, M.; Duarte, I. F.; Almeida, C.; Delgadillo, I.; Goodfellow, B. J.; Gil, A. M.; Morris, G. A. High resolution NMR and diffusion ordered spectroscopy of port wine. *J. Agric. Food Chem.* **2004**, *52*, 3736–3743.
14. Bax, A. A spatially selective composite 90-degrees radiofrequency pulse. *J. Magn. Reson.* **1985**, *65*, 142–145.
15. Bax, A.; Davis, D. G. MLEV-17 based two-dimensional homonuclear magnetization transfer spectroscopy. *J. Magn. Reson.* **1985**, *65*, 355–360.
16. Palmer, A. G.; Cavanagh, J.; Wright, P. E.; Rance, M. Sensitivity improvement in proton detected heteronuclear correlation experiments. *J. Magn. Reson.* **1991**, *93*, 151–170.
17. Schleucher, J.; Schwendinger, M.; Sattler, M.; Schmidt, P.; Schedletzky, O. A general enhancement scheme in heteronuclear multidimensional NMR employing pulsed field gradients. *J. Biomol. NMR* **1994**, *4*, 301–306.
18. Aue, W. P.; Karhan, J.; Ernst, R. R. J. Homonuclear broad band decoupling and two-dimensional J-resolved NMR spectroscopy. *J. Chem. Phys.* **1976**, *64*, 4226–4227.
19. Markley, J. L.; Bax, A.; Arata, Y.; Hilbers, C. W.; Kaptein, R.; Sykes, B. D.; Wright, P. E.; Wuthrich, K. Recommendations for the presentation of NMR structures of proteins and nucleic acids. *Pure Appl. Chem.* **1998**, *70*, 117–142.
20. Lizada, C. Mango. In *Biochemistry of Fruit Ripening*; Seymour, G. B., Taylor, J. E., Tucker, G. A., Eds.; Chapman & Hall: London, 1993; pp. 255–271.
21. Wu, J. S.; Chen, H.; Fang, T. Mango juice. In *Fruit Juice Processing Technology*; Nagy, S., Chen, C. S., Shaw, P. E., Eds.; Agscience: Auburnadale, 1993; pp. 620–655.
22. Tucker, G. A. Introduction. In *Biochemistry of Fruit Ripening*; Seymour, G. B., Taylor, J. E., Tucker, G. A., Eds.; Chapman & Hall: London, 1993; pp. 1–51.
23. Tjan, S. B.; Voragen, A. G. J.; Pilnik, W. Analysis of some partly and fully esterified oligogalactopyranuronic acids by p.m.r. spectrometry at 220 MHz. Carbohydr. Res. **1974**, *34*, 15–23.
24. Neiss, T. G.; Cheng, H. N.; Daas, P. J.H.; Schols, H. A. Compositional heterogeneity in pectic polysaccharides: NMR studies and statistical analysis. *Macromolecules Symposium* **1999**, *140*, 165–178.
25. Belton, P. S.; Delgadillo, I.; Gil, A. M.; Casuscelli, F.; Colquhoun, I. J.; Dennis, M. J.; Spraul, M. High field proton NMR studies of apple juices. *Magn. Reson. Chem.* **1997**, *35*, S52–S60.
26. Medlicott, A. P.; Reynolds, S. B.; Thompson, A. K. Effects of temperature on the ripening of mango fruit (*Mangifera indica* L. var Tommy Atkins). *J. Sci. Food Agric.* **1986**, *37*, 469–474.
27. Angyal, S. J. The composition of reducing sugars in solution. *Adv. Carbohydr. Chem. Biochem.* **1984**, *42*, 15–67.
28. Bock, K.; Thøgersen, H. Nuclear magnetic resonance spectroscopy in the study of mono- and oligosaccharides. *Annu. Rep. NMR Spectrosc.* **1982**, *13*, 1–57.
29. Colquhoun, I. J.; de Ruiter, G. A.; Schols, A.; Voragen, G. J. Identification by NMR spectroscopy of oligosaccharides obtained by treatment of the hairy regions of apple pectin with rhamnogalacturonase. *Carbohydr. Res.* **1990**, *206*, 131–144.

30. Schols, H. A.; Voragen, A. G. J.; Colquhoun, I. J. Isolation and characterization of rhamnogalacturonan oligomers, liberated during degradation of pectic hairy regions of rhamnogalacturonase. *Carbohydr. Res.* **1994**, *256*, 97–111.
31. Tucker, G. A.; Seymour, G. B. Cell wall degradation during mango fruit ripening. *Acta Horticulturae* **1991**, *291*, 454–460.
32. Johnson, C. S. Diffusion ordered nuclear magnetic resonance spectroscopy: principles and applications. *Nucl. Magn. Reson. Spectrosc.* **1999**, *34*, 203–256.
33. Morris, K. F.; Johnson, C. S. Diffusion-ordered 2-dimensional nuclear-magnetic-resonance spectroscopy. *J. Am. Chem. Soc.* **1992**, *114*, 3139–3141.
34. Morris, G. A. Diffusion-ordered spectroscopy (DOSY). In *Encyclopedia of Nuclear Magnetic Resonance*; Grant, D. M., Harris, R. K., Eds.; John Wiley & Sons Ltd: Chichester, 2002; pp. 35–44.